Pergamon

SCIENCE DIRECT®

Tetrahedron 59 (2003) 141–148

TETRAHEDRON

Natural anti-HIV agents. Part 3: Litseaverticillols A–H, novel sesquiterpenes from *Litsea verticillata*☆

Hong-Jie Zhang,[a] Ghee Teng Tan,[a] Vu Dinh Hoang,[b] Nguyen Van Hung,[b] Nguyen Manh Cuong,[c] Djaja Doel Soejarto,[a] John M. Pezzuto[a] and Harry H. S. Fong[a,*]

[a]*Program for Collaborative Research in Pharmaceutical Sciences, College of Pharmacy, University of Illinois at Chicago, 833 S. Wood Street, Chicago, IL 60612, USA*
[b]*Institute of Chemistry, National Center for Science and Technology, Hoang Quoc Viet Str., Gau Giay District, Hanoi, Viet Nam*
[c]*Cuc Phuong National Park, Nho Quan District, Ninh Binh, Viet Nam*

Received 15 November 2001; accepted 18 November 2002

Abstract—Bioassay directed-fractionation led to the identification of litseaverticillols A–H (**1**–**8**) from the leaves and twigs of *Litsea verticillata* Hance. These new sesquiterpenes possess a unique skeleton that was recently designated as 'litseane'. The structures of these compounds were determined by spectroscopic means including 1D and 2D NMR data. Structural configurations were determined by ROESY experiments. Mosher ester reactions and optical rotation measurements established the sesquiterpenes **1**–**8** as racemates. Isolates **1**–**8** inhibited HIV-1 replication in HOG.R5 cells with IC_{50} values ranging from 2 to 15 μg/ml (8–58 μM) while affecting the growth of HOG.R5 at concentrations 2–3-fold higher. Based on this data, structure–activity relationships can be discerned, suggesting compounds of this class are good candidates for analog production.

1. Introduction

Litsea verticillata Hance, a perennial shrub or arbor, was investigated as part of our International Cooperative Biodiversity Group (ICBG) project. This project is designed to address the related issues of biodiversity conservation, economic growth, and promotion of health through the discovery of anti-human immunodeficiency virus (anti-HIV), anti-malarial and anti-tubercular (anti-TB) natural products.[3] Evaluation of the chloroform extract of this plant collected from the Cuc Phuong National Park (Nho Quan District, Ninh Binh Province, Vietnam) demonstrated anti-HIV activity without apparent toxicity to host cells. This extract was prioritized for further phytochemical investigation in view of its capacity to exert a potent in vitro antiviral effect (>80% inhibition at 20 μg/ml) in the absence of interfering polyphenolic compounds such as tannins.

The dried leaves and twigs of *L. verticillata* (4.5 kg) were milled and extracted with MeOH. Subsequent defatting with petroleum ether, followed by partitioning with $CHCl_3$ afforded an active anti-HIV $CHCl_3$ extract (93 g). Bioassay-directed fractionation of the $CHCl_3$ extract by repeated flash column chromatography on silica gel and RP-18, followed by preparative HPLC, afforded eight new litseane sesquiterpenes, litseaverticillols A–H (**1**–**8**). These eight litseane sesquiterpenes constitute members of a novel skeletal type isolated from nature for the first time.[1] Since the structure of litseaverticillol A (**1**) was previously reported,[1] the present paper describes the isolation and structure elucidation of the isolates **2**–**8**, in addition to their anti-HIV activities. A brief discussion of relevant structure–activity relationships is also presented.

2. Results and discussion

Litseaverticillos A–H (Fig. 1) were isolated as colorless gums.

Litseaverticillols A–C (**1**–**3**) showed the same molecular formula of $C_{15}H_{22}O_2$ by the analysis of their HRTOFMS, ^{13}C NMR and DEPT spectra (Table 2). The detailed structural elucidation of litseaverticillol A (**1**) was described previously.[1] Analysis of the ^1H and ^{13}C NMR spectra of litseaverticillol B (**2**) revealed **1** and **2** shared many structural motifs including the α,β-conjugated keto group [δ_C 206.3 (s), 154.8 (d), 142.8 (s)], two double bonds [δ_C 141.8 (s), 132.3 (s), 123.9 (d), 119.7 (d)], and four tertiary methyl groups [δ_H 1.78 (t, J=1.6 Hz), 1.77 (d, J=1.3 Hz), 1.67 (s), 1.61 (s)]. In fact, only two significant differences in the NMR profiles were noted (Tables 1 and 2). The ^{13}C

☆ See Refs. 1,2.

Keywords: *Litsea verticillata*; Lauraceae; litseane; sesquiterpenes; litseaverticillols A–H; anti-HIV activity; bioassay-directed fractionation.

* Corresponding author. Tel.: +1-312-996-5972; fax: +1-312-413-5894; e-mail: hfong@uic.edu

0040–4020/03/$ - see front matter
PII: S0040-4020(02)01491-6

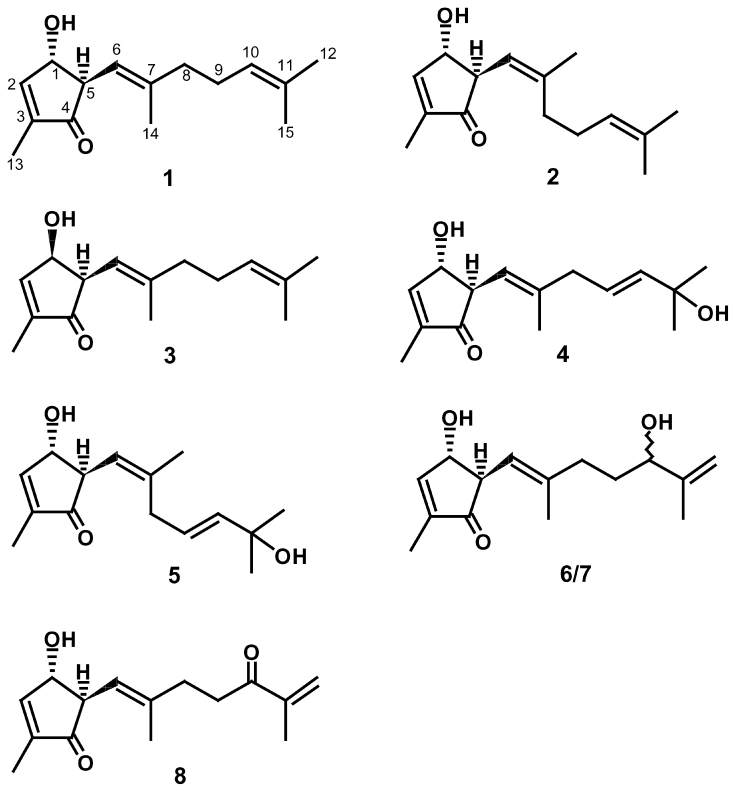

Figure 1. Structures of compounds **1**–**8**.

NMR signal at δ_C 16.97 (q) in **1** was shifted downfield to δ_C 23.3 (q) in **2**, and the signal at δ_C 39.5 (t) in **1** was shifted upfield to δ_C 32.6 (t) in **2**. The two carbons (δ_C 23.3 and δ_C 32.6) in **2** were connected to a double bond ($\Delta^{6,7}$) as evidenced by HMBC spectra (Fig. 2), and assigned as C-8 and C-14, respectively. Analysis of the 2D NMR spectra (^{1}H–^{1}H COSY, HMQC and HMBC) (see Fig. 2 for HMBC data) revealed the ^{13}C chemical shift differences were due to a difference in double bond geometry at $\Delta^{6,7}$ between compounds **1** and **2**. A ROESY cross correlation between H-5 and H-14 (Fig. 3) established that **1** has an *E*-configuration at $\Delta^{6,7}$ which consequently suggested a *Z*-configuration at the same position for **2**. The *Z*-configuration of $\Delta^{6,7}$ in compound **2** was confirmed by the fact that no ROEs between H-5 and H-14 were detected, but instead, the ROEs between H-5 and H-8 were clearly observed. Like **1**, the relative configuration of both chiral carbons in **2** were assigned as R^* due to the small coupling constant between H-1 and H-5. This was caused by the proximate 90° dihedral angle between these two protons.

Table 1. ^{1}H NMR spectral data of compounds **1**–**8** (500 MHz, $CDCl_3$, *J* in Hz)

H	1	2	3	4	5	6/7	8
H-1	4.51, brs	4.53, se[a] (1.9)	4.80, brd (5.8)	4.54, se (2.1)	4.59, se (2.2)	4.54, se (2.1)	4.56, se (1.8)
H-2	7.09, m	7.10, qu[a] (1.5)	7.22, qu (1.5)	7.11, qu (1.6)	7.13, qu (1.4)	7.12, qu (1.7)	7.12, qu (1.6)
H-5	3.10, dd (9.0, 2.4)	3.13, dd (9.5, 2.5)	3.42, dd (8.6, 6.1)	3.12, dd (9.1, 2.4)	3.15, dd (9.1, 2.5)	3.13, dd (9.1, 2.5)	3.14, dd (9.1, 2.4)
H-6	4.95, brd (9.0)	5.00, dq (9.5, 1.2)	4.95, brd (8.5)	4.99, dq (9.1, 1.2)	5.03, dq (9.1, 1.4)	5.02, dq (9.1, 1.3)	5.02, dq (9.1, 1.2)
H-8	2.00, m	2.14, m	2.12, m	2.71, ABdd (15.9, 6.5)	2.79, ABdd, (16.1, 6.8)	2.09, m	2.36, t (7.7)
H-9a		2.17, m	2.15, m				2.85, Abdd (16.4, 7.7)
H-9b		2.10, m	2.10, m				2.79, Abdd (16.4, 7.6)
H-9	2.04, m			5.55, dt (15.6, 6.4)	5.68, dt (15.8, 6.6)	1.63, m	
H-10	5.04, brt (6.7)	5.14, m	5.02, m	5.61, d (15.6)	5.59, dt (15.8, 1.2)	4.02, t (7.9)	
H-12a						4.89, p (0.9)	5.95, brs
H-12b						4.79, p (1.5)	5.76, q (1.1)
Me-12	1.62, s	1.67, s	1.65, s	1.27, s	1.32, s		
Me-13	1.73, t (1.6)	1.78, t (1.6)	1.80, t (1.4)	1.76, t (1.6)	1.79, t (1.6)	1.76, t (1.6)	1.79, t (1.6)
Me-14	1.69, s	1.77, d (1.3)	1.70, d (1.2)	1.68, d (1.3)	1.72, d (1.4)	1.72, d (1.3)	1.74, d (1.2)
Me-15	1.54, s	1.61, s	1.57, s	1.27, s	1.32, s	1.68, brs	1.85, s

[a] se represents sextet; qu represents quintet.

Table 2. ^{13}C NMR spectral data of compounds **1–8** (125 MHz, $CDCl_3$)

C	**1**	**2**	**3**	**4**	**5**	**6/7**	**8**
C-1	76.2 d	76.1 d	69.3 d	76.0 d	76.3 d	76.1 d	76.3 d
C-2	155.6 d	154.8 d	156.2 d	155.6 d	155.1 d	155.5 d	154.9 d
C-3	142.3 s	142.8 s	142.9 s	142.4 s	142.8 s	142.4 s	142.8 s
C-4	206.9 s	206.3 s	207.8 s	206.6 s	206.2 s	206.6 or 206.5 s	206.1 s
C-5	56.0 d	56.3 d	50.9 d	56.2 d	56.3 d	56.2 d	56.2 d
C-6	118.8 d	119.7 d	116.3 d	119.8 d	120.0 d	119.5 or 119.3 d	119.5 d
C-7	141.6 s	141.8 s	144.4 s	140.4 s	140.5 s	141.6 or 141.5 s	140.8 s
C-8	39.5 t	32.6 t	39.6 t	42.1 t	42.4 t	35.8 or 35.7 t	34.2 t
C-9	26. 4 t	26.6 t	26.5 t	124.4 d	129.1 d	32.8 or 32.7 t	36.0 t
C-10	123.8 d	123.9 d	123.7 d	139.8 d	138.1 d	75.5 or 75.3 d	201.6 s
C-11	131.5 s	132.3 s	132.5 s	70.7 s	82.2 s	147.3 or 147.3 s	144.4 s
C-12	25.5 q	25.7 q	25.7 q	29.7 q	24.3 q	111.0 or 110.97 t	124.7 t
C-13	10.1 q	10.2 q	10.2 q	10.2 q	10.2 q	10.2 q	10.2 q
C-14	17.0 q	23.3 q	17.1 q	17.1 q	17.2 q	17.0 or 16.9 q	17.2 q
C-15	17.6 q	17.7 q	17.7 q	29.7 q	24.3 q	17.69 or 17.64 q	17.7 q

Direct evidence for the assignment of a R^*-configuration to H-1 and H-5 was provided by the observation of ROEs between H-1 and H-6 in the ROESY spectrum. Accordingly, **2** was determined to be 1α-hydroxy-(*Z*)-litse-2,6,10-trien-4-one and was given the trivial name of litseaverticillol B.

Litseaverticillol C (**3**) was determined to be an additional analogue of **1** by comparison of their NMR data (Tables 1 and 2). Compound **3** differs from **1** only in the configuration at C-1, which was assigned as S^* in **3** instead of R^* as found in **1**, according to the augmented coupling constant (J=5.8 Hz) between H-1 and H-5, and the absence of ROE correlation between H-1 and H-6 in the ROESY experiments of **3** (Fig. 4). Litseaverticillol C has the same geometric configuration at $\Delta^{6,7}$ as **1** based on the presence of a ROESY correlation between H-5 and H-14. Thus, **3** was determined to be 1β-hydroxy-(*E*)-litse-2,6,10-trien-4-one, and assigned the trivial name litseaverticillol C.

According to their HRTOFMS, ^{13}C NMR and DEPT spectra, litseaverticillols D–G (**4–7**) all have the same molecular formula ($C_{15}H_{22}O_3$), which indicate the presence of one oxygen atom more than found in compounds **1–3**. The similarity in the NMR spectra of **4–7** to those of **1–3** suggested that these compounds also possess the same structural skeleton.

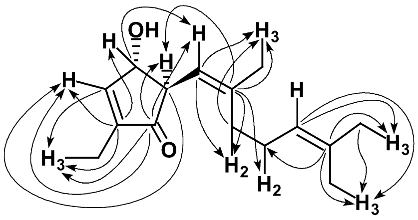

Figure 2. Selected HMBC correlations for compound **2** ($CDCl_3$).

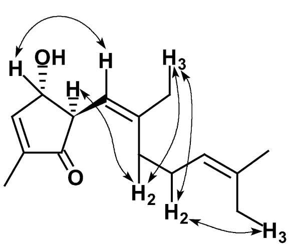

Figure 3. Selected ROESY correlations for compound **2** ($CDCl_3$).

Litseaverticillol D (**4**) gave ^{1}H and ^{13}C NMR signals characteristic of a partial structure consisting of 1-[4-hydroxy-2-methyl-cyclopent-2-en-1-one]-2-methyl-prop-1-enyl [δ_H 7.11 (quintet, J=1.6 Hz), 4.99 (dq, J=9.1, 1.2 Hz), 4.54 (sextet, J=2.1 Hz), 3.12 (dd, J=9.1, 2.4 Hz), 2.71 (ABdd, J=15.9, 6.5 Hz), 1.76 (t, J=1.6 Hz), 1.68 (d, J=1.3 Hz); δ_C 206.6 (s), 155.6 (d), 142.4 (s), 140.4 (s), 119.8 (d), 76.0 (d), 56.2 (d), 42.1 (t), 17.1 (q), 10.2 (q)]. This partial structure is found in compounds **1–3**. A second double bond in **4** was also observed in the ^{1}H and ^{13}C NMR spectra [δ_H 5.61 (d, J=15.6 Hz), 5.55 (dt, J=15.6, 6.4 Hz); δ_C 138.8 (d), 124.4 (d)]. This double bond in **4** was connected directly to the above partial structure to form a 1-[4-hydroxy-2-methyl-cyclopent-2-en-1-one]-2-methyl-penta-1, 4-dienyl (Unit A, Fig. 5) group as evidenced by the ^{1}H–^{1}H COSY correlation between the proton signal at δ 5.55 (dt, J=15.6, 6.4 Hz) and the proton signal at δ 2.71 (ABdd, J=15.9, 6.5 Hz). In addition, there is a 1-hydroxy-1-methylethyl group in **4** [δ_H 1.27 (6H, s); δ_C 70.7 (s), 24.3 (2C, q)] (Tables 1–2). The HMBC correlations (Fig. 5) between C-11 (δ_C 70.7) and H-10 (δ_H 5.61) and between C-11 and H-9 (δ_H 5.55) connected the 1-hydroxy-1-methylethyl group to Unit A, establishing the skeletal structure for **4**. Compounds **4** and **1** have the same

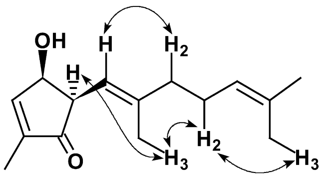

Figure 4. Selected ROESY correlations for compound **3** ($CDCl_3$).

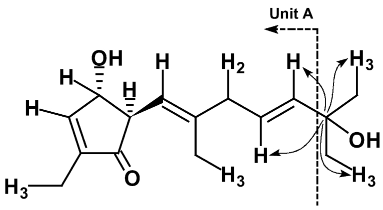

Figure 5. Selected HMBC correlations for compound **4** ($CDCl_3$).

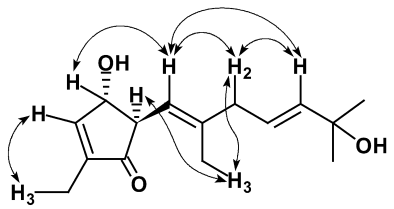

Figure 6. Selected ROESY correlations for compound **4** ($CDCl_3$).

configurations at the two chiral carbons (C-1 and C-5) due to the similar coupling patterns of H-1 and H-5. The large coupling constant (J=15.6 Hz) between H-9 and H-10 in **4** readily established the $\Delta^{9,10}$ double bond to be in an *E*-configuration, while the observed ROE correlation of H-5 and H-14 in the ROESY spectra (Fig. 6) established an *E*-configuration for the $\Delta^{6,7}$ double bond. Thus, compound **4** was determined to be 1α, 11-dihydroxy-(6*E*,9*E*)-litse-2,6,9-trien-4-one, and named litseaverticillol D.

Litseaverticillol E (**5**) was determined to be a geometric isomer of **4** by comparison of their NMR data, with differences occurring at the $\Delta^{6,7}$ double bond. The structural relationship between these two isolates mirrors that between **2** and **1**. The correlation between H-5 and H-8 in the ROESY spectra of **5** (Table 4) indicated a *Z*-configurated $\Delta^{6,7}$ double bond. Thus, litseaverticillol E (**5**) was established as 1α, 11-dihydroxy-(6*Z*,9*E*)-litse-2,6,9-trien-4-one.

Litseaverticillols F and G (**6** and **7**) were isolated as a mixture in a 1:1 ratio. Attempts to separate the two molecules by use of two different HPLC preparative columns (Phenomenex, LUNA phenyl-hexyl, 15 μm, 250×50 mm^2; Grom Saphir 110 C18, 12 μm, 300×40 mm^2) and several different solvent systems were unsuccessful. Separation via Mosher esters were also unsuccessful. Although the ^1H NMR spectra of **6/7** completely overlapped, the ^{13}C NMR signals (Table 2) for 10 of the 15 carbons were clearly separated (maximum difference=0.23 ppm), indicating a mixture of two compounds bearing a close structural relationship. By comparison of the ^{13}C NMR spectral data of **6/7** to **1**, significant differences were found at C-9, C-10, C-11, C-12 and C-15. These positions in **6/7** were comprised of a methylene [δ_H 1.63 (2H, m); δ_C 32.8/32.7 (t)], an oxy-methine [δ_H 4.02 (t, J=7.7 Hz); δ_C 75.5/75.3 (d)], a quaternary olefin [δ_C 147.3/147.2 (s)], an olefinic methylene [δ_H 4.89 (p, J=0.9 Hz) and 4.79 (p, J=1.5 Hz); δ_C 111.0/111.0 (t)] and a tertiary methyl carbons [δ_H 1.68 (3H, brs); δ_C 17.7/17.6 (q)] (Tables 1 and 2), respectively. The absence of an additional methyl NMR signal in **6/7** in conjunction with the presence of a terminal olefinic methylene, suggested a shift of the double bond at $\Delta^{10,11}$ in **1** to $\Delta^{11,12}$ in **6/7**. An extra oxy-methine group in **6/7** was assigned to C-10 due to the HMBC correlations of C-11 to H-12 and H-15, respectively. The geometric and chiral (C-1 and C-5) configurations of **6/7** were determined to be the same as those in **1** due to the similar chemical shifts and coupling patterns at these carbon positions. This conclusion was supported by ROESY spectral data. Thus, **6/7** must be an isomeric pair with differences occurring only at the hydroxyl bearing chiral carbon at C-10. In contrast, C-10 is an olefinic carbon in **1**. That the hydroxyl bearing chiral carbon (C-10) in **6/7** occur on the tail end of a very flexible side chain may explain their occurrence as an inseparable pair. The structures for these two compounds (**6/7**) were assigned as 1α,10α-dihydroxy-(*E*)-litse-2,6,11-trien-4-one and 1α,10β-dihydroxy-(*E*)-litse-2,6,11-trien-4-one, and given the trivial names of litseaverticillols F and G, respectively.

Litseaverticillol H (**8**) was shown to have a molecular formula of $C_{15}H_{20}O_3$ according to HRTOFMS ($[M+Na]^+$ m/z 271.1317), which gave six double bond equivalents; one more than that present in each of the compounds **1**–**7**. The similarity of its NMR data to those of **1**–**7** suggested that **8** was also a litseane sesquiterpene. Compound **8** was determined to be the C-10 oxidation equivalent of **6/7** (δ_C 201.6, C-10) as deduced from analysis of the ^1H–^1H COSY, HMQC and HMBC spectra. The HMBC correlation (Fig. 7) between δ_C 119.5 (d, C-6) and the proton at δ_H 2.36 (2H, t, J=7.7 Hz) established the latter to be H_2-8. The correlation of H_2-8 and the protons at δ_H 2.85 (1H, ABdd, J=16.4, 7.7 Hz) and δ_H 2.79 (1H, ABdd, J=16.4, 7.6 Hz) in turn established these protons as H_2-9. Both H_2-8 and H_2-9 showed long-range coupling with δ_C 201.6 (s) in the HMBC spectra, thus establishing C-10 as a carbonyl carbon. Further evidence for the structural relationship between **6/7** and **8** was established by treatment of **6/7** with pyridinium chlorochromate (PCC)[4] to yield two mono-oxidation products, one of which was identical to **8** by comparison of their ^1H NMR spectra. Therefore, **8** was established as 1α-hydroxy-(*E*)-litse-2,6,11-trien-4,10-dione and assigned the trivial name litseaverticillol H.

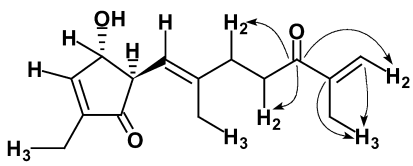

Figure 7. Selected HMBC correlations for compound **8** ($CDCl_3$).

The optical rotations ($[\alpha]_D$) of compounds **1**–**8** were found to be 0°, which suggested they were racemates. Mosher esters prepared from four of these compounds confirmed this suggestion.[5,6] Theoretically, the Mosher reaction of an optically pure compound will result in a single Mosher ester derivative being formed. However, treatment of **1**,[1] **2**, and **4** with (*R*)- or (*S*)-α-methoxy-α-trifluoromethyl-phenylacetyl chlorides (MTPA-Cl) afforded two mono-ester derivatives in approximately 1:1 ratio for each reaction. Thus, **1**, **2**, and **4** were each confirmed to be an equimolar racemic mixture. Mosher esterifications have not been performed for **3**, **5** and **8** due to paucity of material. The Mosher's esters of **6/7** did not yield unequivocal NMR information. However, since the structures of **3**, **5**, **6/7**and **8** are closely related to those of **1**, **2**, and **4**, and their optical rotations were 0°, it is assumed these compounds are also equimolar racemic mixtures.

Compounds **2**–**8** were determined to be closely related in structure to **1**, a prototypic litseane sesquiterpene, recently separated from *L. verticillata*.[1] The ^1H and ^{13}C NMR data of these compounds are very similar to each other (Tables 3 and 4). Compound **2** differs from **1** only by a geometric configuration. Compound **1** possesses an *E*-configuration,

Table 3. Difference of ^{1}H NMR spectral data of compounds **1**–**8** (500 MHz, $CDCl_3$, Δ in ppm)

H	$\Delta^{\delta(2)-\delta(1)}$	$\Delta^{\delta(3)-\delta(1)}$	$\Delta^{\delta(4)-\delta(1)}$	$\Delta^{\delta(5)-\delta(4)}$	$\Delta^{\delta(6/7)-\delta(1)}$	$\Delta^{\delta(8)-\delta(6/7)}$
H-1	+0.02	+0.29	+0.03	+0.05	+0.03	+0.02
H-2	+0.01	+0.13	+0.02	+0.02	+0.03	±0.00
H-5	+0.03	+0.32	+0.02	+0.03	+0.03	+0.01
H-6	+0.05	±0.00	+0.04	+0.04	+0.07	±0.00
H-8	+0.14	+0.12	+0.71	+0.08	+0.09	+0.27
H-9a	+0.13	+0.11				+1.22
H-9b	+0.06	+0.06				+1.16
H-9			+3.51	+0.13	−0.41	
H-10	+0.10	−0.02	+0.57	−0.02	−1.02	
H-12a					+3.27	+1.06
H-12b					+3.17	+0.97
Me-12	+0.05	+0.03	−0.35	+0.05		
Me-13	+0.05	+0.07	+0.03	+0.03	+0.03	+0.03
Me-14	+0.08	+0.01	−0.01	+0.04	+0.03	+0.02
Me-15	+0.07	+0.03	−0.27	+0.05	+0.14	+0.17

whereas **2** has a *Z*-configuration at $\Delta^{6,7}$ which resulted in downfield shifts of all proton signals in the compound, especially those pertaining to the side chain (Table 3). The dramatic upfield shift of the ^{13}C NMR signal of C-8 and the equally dramatic downfield shift of the ^{13}C NMR signal of C-14 in **2** (Table 4) could be explained by the geometric position switch of the two carbons, which led to C-8 in **2** being above the fielding area of the carbonyl group (C-4), and C-14 in **2** being away from the fielding area of the carbonyl group. Compound **3** is an *epi*-isomer of **1**, being epimerized at C-1 by a hydroxyl group. A comparison of the α-OH in **1** with the corresponding β-OH in **3** revealed different ^{1}H NMR coupling patterns of H-1 and H-5. The broad singlet of H-1 in **1** became a broad doublet (J=5.8 Hz) in **3**, and the coupling constant of the doublet of doublets of H-5 were changed from J=9.0, 2.4 Hz in **1** to J=8.6, 6.1 Hz in **3**. Moreover, the epimerization led to significant changes in some NMR chemical shifts, especially those of H-1, H-5, C-1 and C-5 (Tables 3 and 4). In comparison to **1**, compound **4** contains a quaternary hydroxyl group at C-11 and, in addition, the double bond at $\Delta^{10,11}$ in **1** shifted to $\Delta^{9,10}$ in **4**. Besides these apparent NMR chemical shift changes resulting from the different proton and carbon properties (H-9, C-9 and C-11) between **1** and **4**, the structural differences of the two compounds led to other significant NMR data shifts at H_2-8, H-10, H_3-12, H_3-15, C-10, C-12 and C-15 (Tables 3 and 4). The case of the structural difference between **4** and **5** is the same as those between **1** and **2**. Similar to **1** and **2**, almost all of the ^{1}H NMR signals of **5** were shifted downfield from those of **4** (Table 3). However, the differences of the ^{13}C NMR signals between **4** and **5** are unlike the case of **1** and **2**. The ^{13}C NMR chemical shifts of C-8 and C-14 were not dramatically changed between **4** and **5**, as was the case between **1** and **2**. On the other hand, the ^{13}C NMR chemical shifts of C-9, C-11, C-12 and C-15 changed dramatically between **4** and **5** (Table 4). The reason for these changes could be explained by the formation of a hydrogen-bond between the hydroxyl at C-11 and the carbonyl oxygen at C-4 in **5**. This bonding resulted in a dramatic downfield shift of the ^{13}C NMR signal of C-11, and led to a stereo-configuration change of **5**, and causing the two methyl carbons (C-12 and C-15) to be above the fielding area of the carbonyl group, thus generating the upfield shifts of the ^{13}C NMR signals of C-12 and C-15. Compounds **6/7** differed from **1** by having a hydroxyl group at C-11 and the double bond being shifted from $\Delta^{10,11}$ to $\Delta^{11,12}$. This change led to dramatic changes of the NMR chemical shifts of C-8 to C-15. Compound **8** is an oxidized isomer of **6/7**. The oxidation of the 10-OH in **6/7** to a carbonyl group in **8** generated an α,β-conjugated group, which led to significant downfield NMR chemical shifts of H_2-9, H_2-12 and C-12 (Tables 3 and 4).

Isolates **1**–**8** constitute a new class of anti-HIV agents possessing IC_{50} (concentration that inhibits viral replication by 50%) values in the HOG.R5 system ranging from 2 to

Table 4. Difference of ^{13}C NMR spectral data of compounds **1**–**8** (125 MHz, $CDCl_3$, Δ in ppm)

C	$\Delta^{\delta(2)-\delta(1)}$	$\Delta^{\delta(3)-\delta(1)}$	$\Delta^{\delta(4)-\delta(1)}$	$\Delta^{\delta(5)-\delta(4)}$	$\Delta^{\delta(6/7)-\delta(1)}$	$\Delta^{\delta(8)-\delta(6/7)}$
C-1	−0.10	−6.91	−0.17	+0.22	−0.14	+0.26
C-2	−0.78	+0.64	+0.03	−0.51	−0.05	−0.61
C-3	+0.52	+0.65	+0.12	+0.40	+0.18	+0.36
C-4	−0.61	+0.93	−0.31	−0.35	−0.30 or −0.33	−0.50 or −0.47
C-5	+0.30	−5.11	+0.22	+0.09	+0.27	−0.04
C-6	+0.93	−2.47	+1.02	+0.14	+0.68 or +0.47	−0.01 or +0.20
C-7	+0.13	+2.82	−1.19	+0.03	+0.01 or −0.17	−0.82 or −0.64
C-8	−6.96	+0.06	+2.63	+0.22	−3.67 or −3.86	−1.68 or −1.49
C-9	+0.16	+0.08	+97.98	+4.67	+6.40 or +6.23	+3.12 or +3.29
C-10	+0.10	−0.13	+15.96	−1.69	−48.34 or −48.57	+126.07 or +126.30
C-11	+0.83	+0.97	−60.77	+11.43	+15.78 or +15.72	−2.90 or −2.84
C-12	+0.13	+0.10	+4.15	−5.42	+85.49 or +85.43	+13.66 or +13.72
C-13	+0.15	+0.10	+0.09	+0.07	+0.11	+0.04
C-14	+6.37	+0.08	+0.08	+0.12	+0.03 or −0.09	+0.15 or +0.27
C-15	+0.13	+0.12	+12.13	−5.42	+0.13 +0.08	−0.04 or +0.01

Table 5. Anti-HIV activity and cytotoxicity of compounds (**1**–**8**) isolated from *L. verticillata*

Compound	Cytotoxicity to HOG.R5 CC_{50} (μg/ml (μM))	Anti-HIV activity IC_{50} (μg/ml (μM))	SI[a]
1	13.2 (56.2)	5.0 (21.4)	2.6
2	5.7 (24.4)	2–3 (8.5–12.8)	2.8–1.9
3	17.5 (74.8)	7.1 (30.3)	2.4
4	>20 (80)	14.4 (57.6)	>1
5	12.4 (49.6)	4.0 (16)	3.1
6/7	20.0 (80)	11.3 (45.2)	1.7
8	2.5–5.0 (10.1–20.2)	Toxic	–

[a] SI=selectivity index=CC_{50}/IC_{50}.

15 μg/ml (8–58 μM) (Table 5). Thus, it may be noted that change in the geometric configuration at $\Delta^{6,7}$ from *E*- to *Z*-generated a 2–3-fold enhancement in activity between **1** and **2**, and between **4** and **5**. The anti-HIV activity was reduced slightly by the epimerization at C-1 from α to β in **1** and **3**, respectively. With compound **4**, the shift of the double bond from $\Delta^{10,11}$ in **1** to $\Delta,^{9,10}$ and the formation of a hydroxy group at C-11, greatly reduced the anti-HIV activity. This effect was also observed between **2** and **5**. Compounds **6/7** were much less active than **1** due, perhaps, to a double bond shift from $\Delta^{10,11}$ in **1** to $\Delta,^{11,12}$ and the formation of a hydroxy group at C-10. Compared with that of **6/7**, the anti-HIV activity was greatly enhanced in **8** due to the formation of an α,β-conjugated group at C-10 and the presence of $\Delta.^{11,12}$ Nevertheless, the pronounced toxicity of **8** precluded its evaluation as an anti-HIV agent.

Litseaverticillols A–H (**1**–**8**) affected the growth of HOG.R5 cells at CC_{50} (concentration that inhibit cell growth by 50%) values that were 2–3-fold greater than the IC_{50} values for viral inhibition. This generates Selectivity Indices ($SI=CC_{50}/IC_{50}$) in the range of of 2–3. Thus, the anti-HIV activities of **1**–**8** appear moderate since the SI values are sub-optimal. However, distinct structure–activity correlations observed for these compounds render them ideal candidates for analog production in the search for new drug leads.

3. Experimental

3.1. General methods

Optical rotations were measured on a Perkin–Elmer model 241 polarimeter. IR spectra were run on a Jasco FT/IR-410 spectrometer as a film on a KBr plate. 1D and 2D NMR spectra were recorded on a Bruker DRX-500 MHz spectrometer. Chemical shifts (δ) were expressed in ppm with reference to the solvent signals. All NMR data were obtained by using standard pulse sequences supplied by the vendor. Column chromatography was carried out on silical gel (200–400 mesh, Natland International Corporation). Reversed-phase flash chromatography was accomplished with RP-18 silica gel (40–63 μm, EM Science), and reversed-phase HPLC was carried out on a Waters 600E Delivery System pump, equipped with a Waters 996 photodiode detector, and a Watrex GROM-Saphir 110 C18 column (120 Å, 12 μm, 300×40 mm^2) or a Phenomenex LUNA phenyl-hexyl column (120 Å, 15 μm, 250×50 mm^2). Thin-layer chromatography was performed on Whatman glass-backed plates coated with 0.25 mm layers of Silica gel 60. HRTOFMS and MS/MS spectra were recorded on a Micromass QTOF-2 spectrometer.

3.2. Plant material

The initial collection of leaf, twig and flowerbud sample (SVA-0001) of *L. verticillata* Hance (Lauraceae) was made at the Cuc Phuong National Park (CPNP) on November 22, 1998, and was documented by voucher specimens Soejarto et al. 10352. A large amount of the plant sample (SVA-0001, 4.5 kg, voucher specimens Soejarto et al. 11003) was subsequently re-collected at the same site at CPNP on November 17, 1999, for complete isolation work. Duplicate voucher specimens of both collections have been deposited at the herbaria of CPNP, Institute of Ecology and Biological Resources (IEBR at National Center for Science and Technology, Hanoi), and the John G. Searle Herbarium of the Field Museum of Natural History (Chicago, IL, USA).

3.3. Bioassay

Anti-HIV and cytotoxicity assays were performed in parallel utilizing the green fluorescent protein (GFP)-based HOG.R5 reporter cell line that was constructed and developed specifically for quantitating HIV-1 infectivity. The system was validated and adapted as a moderately high-throughput procedure for screening natural products for anti-HIV activity in our laboratory.[2] Briefly, cultures in microtiter wells were infected with HIV-1_{IIIB} (2.5 ng/ml p24) in the presence of plant extracts after which the fluorescence output was measured at the end of 4 days. Virus was omitted from parallel cultures treated with identical concentrations of plant extracts in order to monitor changes in cellular viability by a combination of microscopic and fluorometric measurements.

3.4. Extraction and isolation

The dried and milled leaves and twigs (4.5 kg) were extracted with MeOH, and the extract was subsequently defatted with *n*-hexane and partitioned with $CHCl_3$. The $CHCl_3$-soluble fraction (93.0 g) was chromatographed over a silica gel column (400 g), which was then developed by gradient elution with petroleum ether and increasing concentrations of Me_2CO to afford 16 fractions. Two of these fractions (F-4 and F-5) demonstrated 50% inhibition of HIV-1_{IIIB} infectivity at 20 μg/ml. They were pooled (3.83 g) and subjected to flash column chromatography on a C-18 reverse phase (RP-18, 107 g) column. Subsequent elution with MeOH and H_2O (1:1) yielded an active oily fraction F-17 (1.31 g). F-17 was subjected to preparative

HPLC separation on a GROM-Saphir 110 C18 column (solvent system: MeOH/H_2O 1:1) to afford four active fractions [F34 (123 mg), F35 (70 mg), F39 (147 mg) and F40 (17 mg)], each of which was subjected to further preparative HPLC separation on the GROM-Saphir 110 C18 column. Fraction F34 afforded litseaverticillol D (**4**, 22.8 mg) and litseaverticillols F/H (**6/7**, 34.5 mg) by elution with MeCN/H_2O 3:7. Fraction F35 afforded litseaverticillol E (**5**, 4.2 mg) and litseaverticillol H (**8**, 1.9 mg) by eluting with MeCN/H_2O 4:6. Fraction F39 afforded litseaverticillol C (**3**, 1.6 mg), litseaverticillol A (**1**, 70.6 mg) and litseaverticillol B (**2**, 9.3 mg) when eluted with MeCN/H_2O 6:4.

3.4.1. Litseaverticillol A (1). Colorless gum. For spectral data, see Ref. 1.

3.4.2. Litseaverticillol B (2). Colorless gum, $[\alpha]_D^{20}=0°$ (*c* 0.14, MeOH); UV (MeOH) λ_{max} (log ε)=221 (4.45), 322 (2.98) nm; IR (film) ν_{max}=3371.0 (br), 3018.1, 1713.4, 1671.0, 1646.0, 1446.4, 1377.9, 1327.8, 1228.4, 1153.2, 1033.7, 985.5, 891.9, 848.5, 755.0 cm^{-1}; HRTOFMS *m/z* 257.1520 $[M+Na]^+$ (calcd for $C_{15}H_{22}O_2Na$, 257.1518, Δ +0.2 mmu), 235.1704 $[M+H]^+$ (calcd for $C_{15}H_{23}O_2$, 235.1698, Δ +0.6 mmu); ^1H and ^{13}C NMR data, see Tables 1 and 2.

3.4.3. Litseaverticillol C (3). Colorless gum, $[\alpha]_D^{20}=0°$ (*c* 0.10, MeOH); UV (MeOH) λ_{max} (log ε)=222 (4.48), 323 (3.17) nm; IR (film) ν_{max}=3412.4 (br), 2971.8, 2926.5, 1707.7, 1646.0, 1447.3, 1378.9, 1325.8, 1225.5, 1153.2, 1070.3, 979.7, 911.2, 755.0 cm^{-1}; HRTOFMS *m/z* 257.1521 $[M+Na]^+$ (calcd for $C_{15}H_{22}O_2Na$, 257.1518, Δ +0.3 mmu), 235.1702 $[M+H]^+$ (calcd for $C_{15}H_{23}O_2$, 235.1698, Δ +0.4 mmu); ^1H and ^{13}C NMR data, see Tables 1 and 2.

3.4.4. Litseaverticillol D (4). Colorless gum, $[\alpha]_D^{20}=0°$ (*c* 1.21, MeOH); UV (MeOH) λ_{max} (log ε)=221 (4.34), 320 (2.92) nm; IR (film) ν_{max}=3126.0 (br), 2974.7, 2926.5, 2922.6, 1702.8, 1639.2, 1439.6, 1378.9, 1324.9, 1229.4, 1150.3, 1035.6, 976.8, 929.5, 394.8, 854.3, 759.8 cm^{-1}; HRTOFMS *m/z* 273.1460 $[M+Na]^+$ (calcd for $C_{15}H_{22}O_3Na$, 273.1467, Δ −0.7 mmu), 233.1560 $[M-H_2O+H]^+$ (calcd for $C_{15}H_{21}O_2$, 233.1542, Δ +1.8 mmu), 215.1445 $[M-2H_2O+H]^+$ (calcd for $C_{15}H_{19}O$, 215.1436, Δ +0.9 mmu); TOFMS/MS *m/z* (10 eV, from 233) 233 (100 %), 215 (19), 205 (3), 197 (4),187 (6), 177 (8), 173 (5), 165 (3), 159 (4), 149 (3), 135 (5), 123 (12), 121 (9); TOFMS/MS *m/z* (30 eV, from 233.1560) 233 (6), 215 (5), 204 (11), 200 (17), 185 (50), 171 (22), 167 (34), 157 (72), 145 (84), 143 (61), 135 (45), 131 (61), 121 (100%), 119 (78), 105 (62), 93 (23), 91 (28); ^1H and ^{13}C NMR data, see Tables 1 and 2.

3.4.5. Litseaverticillol E (5). Colorless gum, $[\alpha]_D^{20}=0°$ (*c* 1.21, MeOH); UV (MeOH) λ_{max} (log ε)=222 (4.73), 286 (3.4), 317 (3.30) nm; IR (film) ν_{max}=3190.7 (br), 2915.8, 2852.2, 1707.7, 1458.9, 1377.9, 1322.0, 1228.4, 1153.2, 1043.3, 979.7, 755.0 cm^{-1}; HRTOFMS *m/z* 273.1470 $[M+Na]^+$ (calcd for $C_{15}H_{22}O_3Na$, 273.1467, Δ +0.3 mmu); ^1H and ^{13}C NMR data, see Tables 1 and 2.

3.4.6. Litseaverticillol F/G (6/7). Colorless gum, $[\alpha]_D^{20}=0°$ (*c* 1.79, MeOH); UV (MeOH) λ_{max} (log ε)=223 (4.11), 320 (3.01) nm; IR (film) ν_{max}=3271.6 (br), 3072.1, 2991.1, 2910.1, 1701.9, 1646.0, 1448.3, 1383.7, 1322.0, 1228.4, 1165.8, 1034.6, 985.5, 899.6, 854.3, 756.0 cm^{-1}; HRTOFMS *m/z* 273.1482 $[M+Na]^+$ (calcd for $C_{15}H_{22}O_3Na$, 273.1467, Δ +1.5 mmu); ^1H and ^{13}C NMR data, see Tables 1 and 2.

3.4.7. Litseaverticillol H (8). Colorless gum, $[\alpha]_D^{20}=0°$ (*c* 0.11, MeOH); UV (MeOH) λ_{max} (log ε)=221 (4.66), 317 (3.13) nm; IR (film) ν_{max}=3427.9 (br), 2923.6, 2854.1, 1732.7, 1708.6, 1651.7, 1458.9, 1377.9, 1228.4, 1072.2, 1035.6, 942.1, 755.0 cm^{-1}; HRTOFMS *m/z* 271.1317 $[M+Na]^+$ (calcd for $C_{15}H_{20}O_3Na$, 271.1310, Δ +0.7 mmu); ^1H and ^{13}C NMR data, see Tables 1 and 2.

3.5. Preparation of Mosher's esters

To a solution of 1.0 mg of isolate in 0.3 mL of dry pyridine was added sequentially 4-(dimethylamino)-pyridine (1.0 mg) and (*R*)-(+)-α-methoxy-α-trifluoromethylphenylacetic chloride (10 μL, MTPACl). After stirring the mixture under N_2 at room temperature for 12 h, 5% $NaHCO_3$ (2 mL) and $CHCl_3$ (5 mL) were added. Vigorous stirring was carried out for 5 min to allow efficient hydrolysis of the excess MTPA-Cl. The organic phase was washed with 0.5N HCl, dried over anhydrous Na_2SO_4, and concentrated to yield a yellow gum. This gum was purified by semi-preparative HPLC separation on a GROM-SIL ODS column (120 Å, 5 μm, 300×20 mm^2) and eluted with MeCN/H_2O 8:2 to yield (*S*)-MTPA esters. The use of (*S*)-(+)-α-methoxy-α-trifluoromethylphenylacetic chloride gave (*R*)-MTPA esters. Work-up of the reaction product of **2** with (*S*)-MTPACl gave the (*R*)-Mosher's esters. In the same manner, **4** yielded a pair of (*S*)-Mosher's esters by reacting with (*R*)-MTPACl. Each pair of Mosher's esters were obtained in a ca. 1:1 ratio according to the ^1H NMR spectra in yields of 70–80%. The Mosher esterification of **1** was reported previously.[1]

3.5.1. (*R*)-MTPA esters of 2. ^1H NMR (500 MHz, $CDCl_3$, *J* in Hz) δ 7.50–7.45 (4H, m, aromatic), 7.42–7.35 (6H, m, aromatic), 7.16 (1H, m, H-2), 7.10 (1H, m, H-2), 5.72 (2H, brs, H-1), 5.33 (2H, m, H-10), 5.05 (1H, brd, *J*=9.4 Hz, H-6), 4.99 (1H, brd, *J*=9.1 Hz, H-6), 3.53 (3H, s, OMe), 3.51 (3H, s, OMe), 3.35 (1H, dd, *J*=9.6, 2.1 Hz, H-5), 3.25 (1H, brd, *J*=9.1 Hz, H-5), 2.40–2.20 (4H, m, H-9), 2.08-1.90 (4H, m, H-8), 1.86 (3H, s, Me-13), 1.83 (3H, s, Me-13), 1.78 (3H, s, Me-14), 1.75 (3H, s, Me-14), 1.64 (6H, s, Me-12).

3.5.2. (*S*)-MTPA esters of 4. ^1H NMR (500 MHz, $CDCl_3$, *J* in Hz) δ 7.60–7.40 (10H, m, aromatic), 7.18 (1H, m, H-2), 7.11 (1H, m, H-2), 5.73 (2H, m, H-1), 5.66 (2H, d, *J*=15.6 Hz, H-10), 5.59 (2H, dt, *J*=15.5, 6.3 Hz, H-9), 5.04 (1H, brd, *J*=10.2 Hz, H-6), 5.02 (1H, brd, *J*=10.1 Hz, H-6), 3.54 (3H, s, OMe), 3.51 (3H, s, OMe), 3.35 (1H, dd, *J*=9.5, 2.2 Hz, H-5), 3.24 (1H, dd, *J*=9.4, 2.3 Hz, H-5), 2.76 (2H, ABm, H-8), 2.73 (2H, ABm, H-8), 1.84 (3H, s, Me-13), 1.82 (3H, s, Me-13), 1.29 (12H, s, Me-12/Me-15).

3.5.3. Oxidation of 6/7 with PCC. Pyridinium chlorochromate (PCC, 5 mg) was suspended in CH_2Cl_2 (2 mL), and the isolated mixture, **6/7** (2 mg in 1 mL of CH_2Cl_2), was rapidly

added at room temperature. After 1 h, the reaction mixture was diluted with 10 mL of ether. The solvent was decanted, and the solid residue was washed twice with ether (5 mL). The combined solution was evaporated to dry to afford a mixture, which was subjected to semipreparative HPLC separation on the GROM-SIL ODS column (120 Å, 5 μm, 300×20 mm^2) and an elution solvent of MeCN/H_2O 4:6 to afford two compounds. One (0.31 mg) showed an identical ^1H NMR spectrum with that of **8**. The second compound (0.18 mg) was elucidated as 1-oxo-litseaverticillols F and G according to ^1H NMR spectrum (500 MHz, $CDCl_3$, *J* in Hz) δ 6.98 (1H, brs, H-2), 4.92 (1H, brs, H-12a), 4.89 (1H, brd, *J*=7.9 Hz, H-6), 4.81 (1H, brs, H-12b), 4.30 (1H, brt, *J*=6.3 Hz, H-10), 3.63 (1H, d, *J*=8.6 Hz, H-5), 2.15 (2H, m, H_2-8), 2.10 (3H, s, Me-13), 1.77 (3H, s, Me-14), 1.70 (3H, s, Me-15), 1.67 (2H, m, H_2-9).

Acknowledgements

All work involving plant sample collection, taxonomic identification, bioassay-guided chemical isolation, and structure elucidation in connection with this paper were carried out under a grant administered by the Fogarty International Center, NIH (Grant 1 UO1-TW01015-01), as part of an International Cooperative Biodiversity Group (ICBG) program. The authors are grateful to the Research Resources Center, University of Illinois at Chicago for access to the Bruker DRX 500 MHz instrument, and to the Center Research Group of the College of Pharmacy, University of Illinois at Chicago for the acquisition of MS data. The authors also wish to acknowledge the AIDS Research and Reference Reagent Program, NIAID, NIH for the supply of reagents critical to this study.

References

1. Zhang, H. J.; Tan, G. T.; Hoang, V. D.; Hung, N. V.; Cuong, N. M.; Soejarto, D. D.; Fong, H. H. S.; Pezzuto, J. M. *Tetraheron Lett.* **2001**, *42*, 8587–8591.
2. Hoang, V. D.; Tan, G. T.; Zhang, H. J.; Tamez, P. A.; Hung, N. V.; Xuan, L. X.; Huong, L. M.; Cuongm, N. M.; Thao, D. T.; Soejarto, D. D.; Fong, H. H. S.; Pezzuto, J. M. *Phytochemistry* **2002**, *59*, 325–329.
3. Soejarto, D. D.; Gyllenhaal, C.; Regalado, J. C.; Pezzuto, J. M.; Fong, H. H. S.; Tan, G. T.; Hiep, N. T.; Xuan, L. T.; Binh, D. Q.; Hung, N. V.; Bich, T. Q.; Thin, N. N.; Loc, P. K.; Vu, B. M.; Southavong, B. H.; Sydara, K.; Bouamanivong, S.; O'Neill, M. J.; Lewis, J.; Xie, X.; Dietzman, G. *Pharm. Biol.* **1999**, *37*(Suppl), 100–113.
4. Corey, E. J.; Suggs, J. W. *Tetrahedron Lett.* **1975**, 2647–2650.
5. Dale, J. A.; Mosher, H. S. *J. Am. Chem. Soc.* **1973**, *95*, 512–519.
6. Ohtani, I.; Kusumi, T.; Kashman, Y.; Kakisawa, H. *J. Am. Chem. Soc.* **1991**, *113*, 4092–4096.